Journal of Chromatography A, 1217 (2010) 2197–2205

Contents lists available at ScienceDirect

Journal of Chromatography A

journal homepage: www.elsevier.com/locate/chroma

Development of mesoporous TiO_2 microspheres with high specific surface area for selective enrichment of phosphopeptides by mass spectrometric analysis

Jia Tang[a], Peng Yin[a], Xiaohui Lu[b], Dawei Qi[a], Yu Mao[c], Chunhui Deng[a,*], Pengyuan Yang[a], Xiangmin Zhang[a,*]

[a] Department of Chemistry & Institutes of Biomedical Sciences, Fudan University, 220 Handan Road, Shanghai 200433, China
[b] Center of Analysis and Measurement, Fudan University, Shanghai 200433, China
[c] Center of Evaluation for Drug Safety, Second Military Medical University, Shanghai 200433, China

ARTICLE INFO

Article history:
Received 2 December 2009
Received in revised form 30 January 2010
Accepted 2 February 2010
Available online 11 February 2010

Keywords:
Mesoporous TiO_2 microspheres
Phosphopeptide enrichment
Mass spectrometry

ABSTRACT

In this study, mesoporous TiO_2 microspheres were synthesized by simple hydrothermal reaction, and successfully developed for phosphopeptides enrichment from both standard protein digestion and real biological sample such as rat brain tissue extract. The mesoporous TiO_2 microspheres (the diameter size of about 1.0 μm) obtained by simple hydrothermal method were found to have a specific surface area of 84.98 m^2/g, which is much larger than smooth TiO_2 microspheres with same size. The surface area of mesoporous TiO_2 microspheres is almost two times of commercial TiO_2 nanoparticle (a diameter of 90 nm). Using standard proteins digestion and real biological samples, the superior selectivity and capacity of mesoporous TiO_2 microspheres for the enrichment of phosphorylated peptides than that of commercial TiO_2 nanoparticles and TiO_2 microspheres was also observed. It has been demonstrated that mesoporous TiO_2 microspheres have powerful potential for selective enrichment of phosphorylated peptides. Moreover, the preparation of the mesoporous TiO_2 microspheres obtained by the hydrothermal reaction is easy, simple and low-cost. These mesoporous TiO_2 microspheres with the ability of large scale synthesis can widely be applied for phosphorylated proteomic research.

© 2010 Elsevier B.V. All rights reserved.

1. Introduction

Protein phosphorylation is one of the most widespread regulatory mechanisms in nature. This mechanism controls a wide variety of cellular events, including metabolism, transcriptional, and translational regulation, degradation of proteins, homeostasis, cellular signaling and communication, proliferation, differentiation, and cell survival [1,2]. To achieve detailed insights into phosphorylation-controlled cellular regulation, it is important to identify phosphorylated proteins and to determine the precise sites of phosphorylation within those proteins as well as the phosphorylation residency at a certain metabolic stage [3]. Mass spectrometry, including electrospray ionization-mass spectrometry (ESI-MS) and matrix-assisted laser desorption/ionization-mass spectrometry (MALDI-MS), has been widely applied as a powerful tool to characterize protein modifications, including phosphorylation, due to its high sensitivity and capability of rapid sequencing by tandem mass spectrometric (MS^n) techniques [4–9]. However, the identification and characterization of phosphoprotein by mass spectrometry is still a challenging task because of commonly low occurrence of phosphorylation in biological sample as well as the suppression effect of phosphopeptides signals by nonphosphorylated peptide residues contained in the protein digest. Therefore, prior isolation and enrichment of phosphopeptides from a proteolytic peptide mixture are often required.

There are several strategies used for specific capture of phosphopeptides, including immobilized metal ion affinity chromatography (IMAC) incorporating Ti^{4+}, Fe^{3+}, Ga^{3+}, Al^{3+}, or Co^{2+} [10–14], immunoprecipitation with phosphoprotein-specific antibodies [15,16], the addition of an affinity tag to phosphorylated amino acids through chemical reactions [17,18], and chromatography separation [19–23]. Among all these strategies, IMAC method is the most widely used both on-line and off-line. Recently, metal oxide chromatography was introduced as an alternative to IMAC. For example, metal oxides such as titania and zirconia [24–31] have also been used to selectively concentrate phosphopeptides, where the phosphate functional groups can bind to the surface of metal oxide particles. Because of their stability over a wide pH range, acid buffers can be employed to avoid non-specific binding. Other than chromatography separation methods, various rapid phosphopeptides enrichment strategies have been developed using metal ions or metal oxides micro/nano-particles [32,33]. Our lab has also developed a series of metal oxides functionalized

* Corresponding authors. Tel.: +86 21 65643983; fax: +86 21 65641740.
E-mail addresses: chdeng@fudan.edu.cn (C. Deng), xmzhang@fudan.edu.cn (X. Zhang).

0021-9673/$ – see front matter © 2010 Elsevier B.V. All rights reserved.
doi:10.1016/j.chroma.2010.02.008

magnetic core–shell microspheres for rapid and high specific capture of phosphopeptides [34–38]. Despite the diversity of enrichment strategies, TiO_2 is the most commonly used metal oxides for selective capture of target peptides since it is extremely tolerant toward most buffers and salts used in biochemistry and cell biology laboratories [39–42]. New improved procedures [43–47] were reported for the purification of phosphopeptides peptides using TiO_2 materials. Recently, mesoporous materials with large pore size and high specific surface area are of particular interest for proteomics. Yang and coworkers [48] applied mesoporous silica materials to immobilize enzyme for protein fast digestion for proteome research. Zou and coworkers [49] developed highly ordered mesoporous silica for selective enrichment of peptides in biological samples. More recently, Zou et al. used mesoporous organosilicas particles as supports for further modification by phosphonic acid or metal ions. These functionalized mesoporous particles were successfully developed as new IMAC materials for phosphorylated peptides enrichment [33,50]. High surface area and unique mesoporous structure contribute to more efficient affinity selectivity and capacity [49,50], therefore, the development of mesoporous metal oxides especially mesoporous TiO_2 for phosphopeptide enrichment is very interesting, and very important for phophoproteomics. However, to our knowledge, few papers concerning using mesoporous TiO_2 materials for selective enrichment of phosphopeptides in biological samples are reported [51].

In this paper, we synthesized mesoporous TiO_2 microspheres with a high surface area to volume ratio using simple hydrothermal reaction [52], and applied to selective enrichment of phosphopeptides in standard protein digestion and real biological samples. Compared with the TiO_2 microspheres with a smooth surface, the surface area of mesoporous TiO_2 microspheres is approximately 25 times as much as that of smooth TiO_2 microspheres. Both of these two materials are successfully applied to selective phosphopeptides enrichment from standard protein digest such as β-casein. However, when they are used for phosphopeptides enrichment from complicated samples like standard protein digest mixture or proteolytic peptide mixture generated from biological sample, mesoporous TiO_2 microspheres exhibit higher specific capture ability compared with smooth TiO_2 microspheres due to their massive surface area. Commercial available TiO_2 nanospheres with a diameter of 90 nm were also used for phosphopeptide enrichment from digestion products of rat brain tissue extract. 223, 47 and 90 phosphopeptides were identified by mesoporous, smooth and commercial TiO_2 materials, respectively. Mesoporous TiO_2 microspheres exhibit higher specific capture ability compared with other TiO_2 particle counterparts due to their high surface area. The synthesis of TiO_2 microsphere with mesoporous surface is easy and low-cost, and it holds great promises to be used as chromatographic materials for phosphopeptide enrichment.

2. Materials and methods

2.1. Reagents

Bovine β-casein, chicken egg albumin (ovalbumin), bovine serum albumin, L-1-tosylamido-2-phenylethyl chloromethyl ketone (TPCK) treated trypsin (from bovine pancreas), ammonium hydrogen carbonate (NH_4HCO_3), dithiothreitol (DTT), iodoacetamide, trifluoroacetic acid (TFA) and 2,5-dihydroxybenzoic acid (DHB) were purchased from Sigma USA (St. Louis, MO, USA). Acetonitrile was purchased from Merck (Darmstadt, Germany). All aqueous solutions were prepared using Milli-Q water by Milli-Q system (Millipore, Bedford, MA, USA). All other reagents were of analytical grade and were purchased from Shanghai Chemical Reagent. Commercial anatase TiO_2 particles with a diameter of 90 nm were purchased from Hisun Technology Co., Ltd. (Zhoushan, Zhejiang Province, P.R. China).

2.2. Preparation and characterization of mesoporous and smooth TiO_2 microspheres

2.2.1. Synthesis of mesoporous and smooth TiO_2 microspheres

Mesoporous and smooth TiO_2 microspheres were synthesized according to the previous method [52]. Briefly, HAD (hexadecylamine) was dissolved in ethanol followed by the addition of KCl solution (0.1 M). TIP (titanium (IV) isopropoxide) was added into this solution under vigorous stirring at ambient temperature. The resulting white TiO_2 suspension was kept static at the same temperature for 18 h, and the obtained TiO_2 appeared to be amorphous. These TiO_2 beads had smooth surface and were used as contrast in phosphopeptides enrichment experiments. In order to obtain the mesoporous TiO_2 beads with a highly crystalline framework, the amorphous TiO_2 beads were collected on a Millipore filter, washed with ethanol three times and dried in air at room temperature. Then a solvothermal process was used. Amorphous TiO_2 beads were dispersed into a mixture of ethanol and deionized water, then 25% ammonia solution were added. The mixtures were sealed within a Teflon-lined autoclave and heated at 160 °C for 16 h. The solid products were collected by filtration, washed with ethanol, and dried in air at room temperature. The resultant powders were calcined at 500 °C for 2 h in air to remove organic components and produce the final mesoporous TiO_2 beads for characterization.

2.2.2. Characterization

Scanning electron microscopy (SEM) images were obtained using a JEOL JSM-6500F SEM instrument. Transmission electron microscopy (TEM) images were obtained using a JEOL JEM-2010 TEM instrument. XRD measurements were performed on a Rigaku D/MAXIIA X-ray diffractometer using Cu Kα radiation. Nitrogen adsorption–desorption measurements were performed on a Micromeritics Tristar 3000 system at 77 K.

2.3. Sample preparation

Bovine β-casein and bovine serum albumin were dissolved in 25 mM NH_4HCO_3 buffer at pH 8.3 (1 mg/mL for each protein) and treated with trypsin (2%, w/w) for 16 h at 37 °C, respectively. The resulting peptide mixtures were stored at −20 °C until further use. All the peptide mixtures were diluted with binding buffer before use.

Rats were sacrificed and the brains were promptly removed and placed in ice-cold homogenization buffer consisting of 8 M urea, 4% CHAPS (w/v), 65 mM 1,4-dithiothreitol (DTT), 1 mM ethylenediaminetetraacetic acid, 0.5 mM ethylene glycol tetraacetic acid, and a mixture of protease inhibitor (1 mM phenylmethanesulphonylfluoride) and phosphatase inhibitors (0.2 mM Na_3VO_4, 1 mM NaF) and 40 mM Tris–HCl at pH 7.4. After mincing with scissors and washing with PBS to remove blood, the brain tissues were homogenized in a Pottter-Elvejhem homogenizer with a Teflon piston, using 4 mL of the homogenization buffer per 1 g of tissue. The suspension was homogenized for approximately 2 min, vortexed at 0 °C for 30 min, and centrifuged at 16,000 × *g* for 40 min. The supernatant was then collected for trypsin digestion. Protein concentration was measured by the Bradford assay, using BSA as a standard protein. For trypsin digestion, 1 M NH_4HCO_3 buffer was added into the supernatant to reach a final concentration of 25 mM first. The protein solution was reduced with 10 mM DTT for 30 min at 56 °C, and then alkylated with 100 mM iodoacetamide for 30 min at 37 °C. After alkylation, the protein mixture was incubated with trypsin (50:1) at 37 °C overnight. Resulted peptide solution was

used for further experiment immediately or stored at −20 °C until use.

2.4. Selective enrichment of phosphopeptides with TiO_2 microspheres

The peptide mixtures originating from tryptic digestions were diluted to a certain concentration by binding buffer first. Suspensions of TiO_2 microspheres (20 μL of 2 μg/μL) were added into 200 μL diluted peptide mixture for selective enrichment. The mixed solutions were vibrated at 25 °C for 30 min. After that, the supernatants were discarded after centrifugation, and remained TiO_2 microspheres were washed with binding buffer for three times. Then the obtained peptide-loaded microspheres were redispersed in 5 μL 0.4 M ammonia aqueous solution for MALDI-MS analysis.

For phosphopeptide enrichment of peptide mixture digested from the rat brain tissue lysate, the peptide solution was first diluted four times with binding buffer. 1 mg of mesoporous, smooth TiO_2 microspheres and 90 nm commercial TiO_2 nanoparticles were mixed with 500 μL lysate, respectively. Following binding, washing and elution steps were the same as standard protein digests. Finally the eluates were lyophilized and then dissolved with 40 μL 5% ACN in 0.1% formic acid, and submitted for nano-RPLC-ESI-MS/MS analysis.

2.5. MALDI-MS analysis

The enriched phosphopeptides from standard proteins eluted from TiO_2 microspheres were deposited on the MALDI target using dried droplet method. 0.5 μL of the washing buffer was deposited on the plate and then another 0.5 μL of a mixture of 20 mg/mL 2,5-dihydroxybenzoic acid in 50% acetonitrile and 1% H_3PO_4 aqueous solution (v/v) was introduced as a matrix. MALDI-TOF MS experiments were performed in positive ion mode on a 4700 Proteomics Analyzer (Applied Biosystems, USA) with the Nd-YAG laser at 355 nm, a repetition rate of 200 Hz and an acceleration voltage of 20 kV. All spectra were taken from signal-averaging of 800 laser shots with the laser intensity kept at a proper constant.

2.6. Automated nano-flow RPLC-ESI-MS/MS analysis

Nano-LC MS/MS experiment was performed on an HPLC system composed by 2 LC-20AD nano-flow LC pumps and 1 LC-20AB micro-flow LC pump (all from Shimadzu Corporation, Tokyo, Japan) connected to an LTQ mass spectrometer (Thermo Electron Corporation, San Jose, CA, USA). Sample injection was done via an SIL-20 AC auto-sampler (Shimadzu Corporation, Tokyo, Japan) and loaded onto a CAPTRAP column (0.5 mm × 2 mm, MICHROM Bioresources Inc., Auburn, CA) for 5 min at a flow rate of 60 μL/min. The sample was subsequently separated by a PICOFRIT C18 reverse-phase column (0.075 mm × 100 mm, New Objective Inc., Woburn, MA) at a flow rate of 300 nL/min. The mobile phases consisted of 5% acetonitrile with 0.1% formic acid (phase A and the loading phase) and 95% acetonitrile with 0.1% formic acid (phase B). To achieve proper separation, a 120-min linear gradient from 5 to 45% phase B was employed. The separated sample was introduced into the mass spectrometer via a 15 μm silica tip (New Objective Inc., Woburn, MA) adapted to a DYNAMIC nano-electrospray source (Thermo Electron Corporation, San Jose, CA). The spray voltage was set at 2.0 kV and the heated capillary at 210 °C. The mass spectrometer was operated in data-dependent mode and each cycle of duty consisted one MS survey scan at the mass range 400–2000 Da, followed by MS2 experiments for 8 strongest peaks and MS3 experiment for the peak corresponding to the neutral loss of 97.97, 48.99, 32.67 Da among the three most intense fragment ions using the LTQ section. Peptides were fragmented in the LTQ section using collision-induced dissociation with helium and the normalized

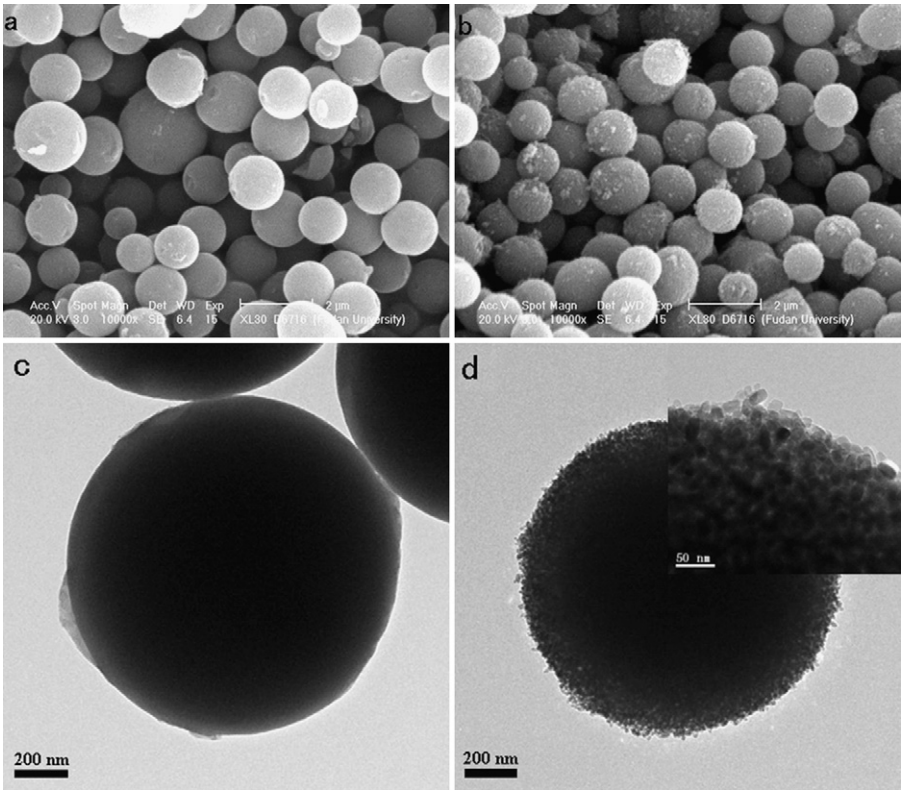

Fig. 1. SEM and TEM images of the smooth (a, c) and mesoporous TiO_2 microspheres (b, d).

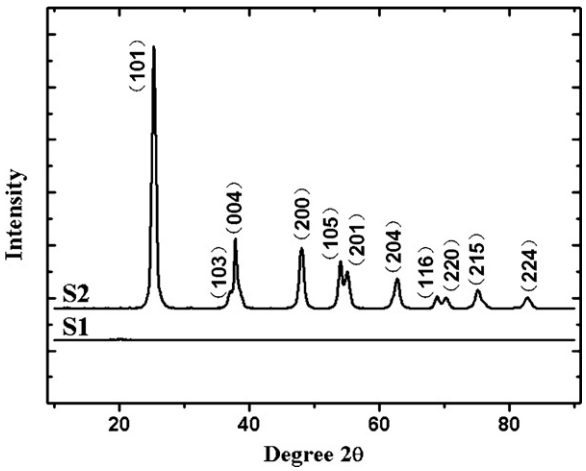

Fig. 2. XRD patterns of the smooth amorphous (sample S1) and mesoporous anatase (sample S2) TiO_2 microspheres.

collision energy value set at 35%. Previously fragmented peptides were excluded for 30 s.

2.7. Peptide sequencing and data interpretation

The mass spectra were searched against the International Protein Index (IPI) database (IPI rat v3.45 fasta with 40 189 entries) using the Bioworks software (Version 3.3.1; Thermo Electron Corp.) based on the SEQUEST algorithm. The parameters for the SEQUEST search were as follows: enzyme, partialTrypsin; missed cleavages, one; fixed modification, carboxyamidomethylation (C); variable modifications, phosphorylation (S, T, Y) and oxidation (M); peptide tolerance, 3.0 Da; MS/MS tolerance, 1.0 Da. The database search results were statistically analyzed using PeptideProphet [53], which effectively computes a probability for generating statistical validation of MS/MS search engines' spectra-to-peptide sequence assignments. A minimum PeptideProphet probability score filter of 0.95 was used to remove low-probability peptides.

3. Results and discussion

3.1. Characterization of amorphous and mesoporous anatase TiO_2 microspheres

A series of characterization methods were taken in order to conform the structures of TiO_2 microspheres. Fig. 1a and b shows scanning electron microscopy (SEM) images of the amorphous and mesoporous TiO_2 microspheres, respectively, illustrating the uniform size distribution of the microspheres. Amorphous TiO_2 microspheres possess very smooth surfaces while mesoporous TiO_2 microspheres have obvious granular features, which can be observed clearly from the TEM images presented at Fig. 1c and d. The corresponding X-ray diffraction (XRD) patterns (Fig. 2) have further proved the amorphous and anatase structures of these two materials. The XRD pattern of the mesoporous TiO_2 microspheres (Fig. 2) showed well-resolved diffraction peaks corresponding to the reflections of anatase TiO_2 material (JCPDS card No. 21-1272).

The specific surface areas and pore size distributions of the smooth and mesoporous TiO_2 microspheres have been characterized using nitrogen gas sorption and are shown in Fig. 3. A hysteresis loop was observed for the mesoporous TiO_2 microspheres in Fig. 3a, indicating their relatively large pore sizes. According to Fig. 3b, the specific surface area of mesoporous material was 84.98 m^2/g, while the surface area of amorphous material was only 3.35 m^2/g and there was no obvious porous characteristic shown in the corresponding pore size distribution curve. Commercial TiO_2 nanoparticles were also taken for BET characterization. The specific surface area was 47.17 m^2/g (data not shown). These characterization data have further confirmed the formation and the specific surface area of the synthesized amorphous and mesoporous anatase TiO_2 microspheres.

3.2. Optimization of TiO_2 microspheres phosphopeptide enrichment conditions

Titanium oxide can react either as a Lewis acid or base depending on the pH of the reaction solution. In acidic solution, TiO_2 behaves as a Lewis acid with positively charged titanium atoms, thereby displaying anion-exchange properties. High binding affinity for polyoxy anions, including phosphate, borate, carboxylate, and sulfate has been demonstrated [54]. The markedly high binding constant of phosphate ions suggesting that high binding selectivity of phosphorylated peptides over nonphosphorylated peptides should be achieved upon appropriate condition. Fig. 4a–f shows the direct MALDI mass spectrum of enriched tryptic digest of β-casein (1 ng/μL) using mesoporous anatase TiO_2 microspheres under different binding conditions. All these enrichment experiments involved washing and elution in 0.4 M NH_4HCO_3. Identified phosphopeptides are labeled with numbers from 1 to 9 and included in Table 1. The signals stand for metastable loss of phosphoric acid from adjacent parent ions are labeled with asterisks. Spectra obtained under binding buffer consisting of pure water or 50% ACN solution showed severe interference from nonphosphorylated peptides as shown in Fig. 4a and c. Therefore it is critical to use

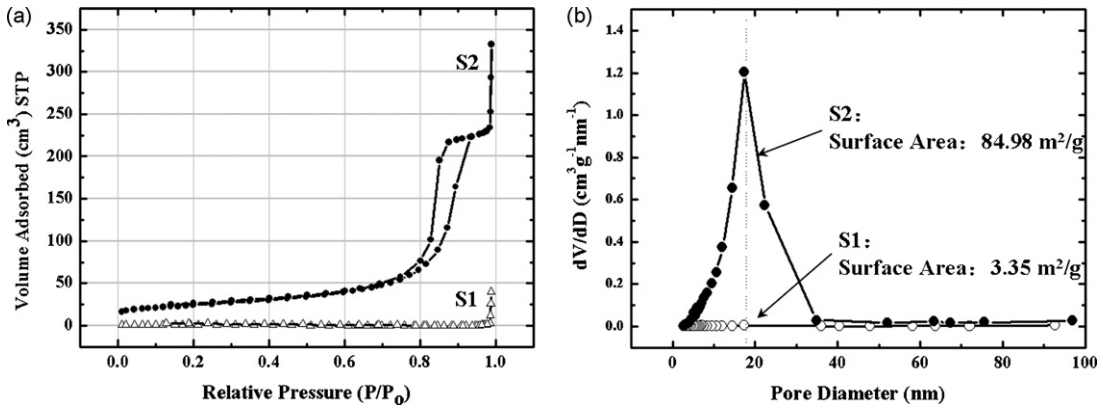

Fig. 3. (a) Nitrogen sorption isotherms of the smooth amorphous (sample S1) and mesoporous anatase (sample S2) TiO_2 microspheres. (b) Pore diameter distribution of the smooth amorphous (sample S1) and mesoporous anatase (sample S2) TiO_2 microspheres.

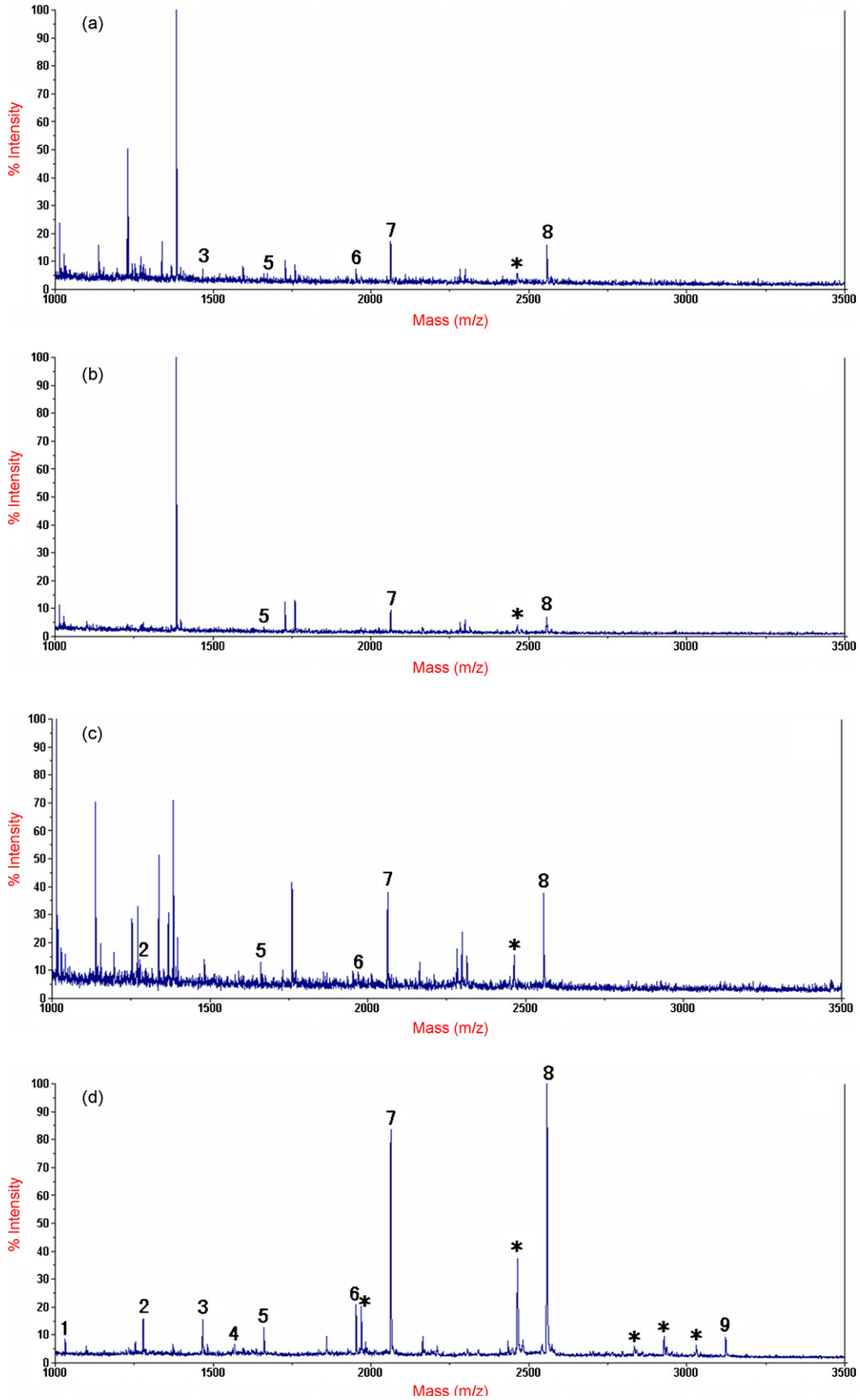

Fig. 4. Mass spectra obtained using the mesoporous anatase TiO_2 microspheres to selectively enrich phosphorylated peptides from the tryptic digest of β-casein at concentration of 4.4×10^{-7} M under bind buffer (a) pure water, (b) 0.2% TFA, (c) 50% ACN, (d) 0.2% TFA and 50% ACN, (e) 2% TFA and 50% ACN, (f) 0.2% TFA and 80% ACN, respectively. All spectra were taken from signal-averaging of 800 laser shots with the laser intensity kept at a proper constant. Phosphopeptides ions identified are marked with numbers. The metastable losses of phosphoric acid are indicated with asterisks.

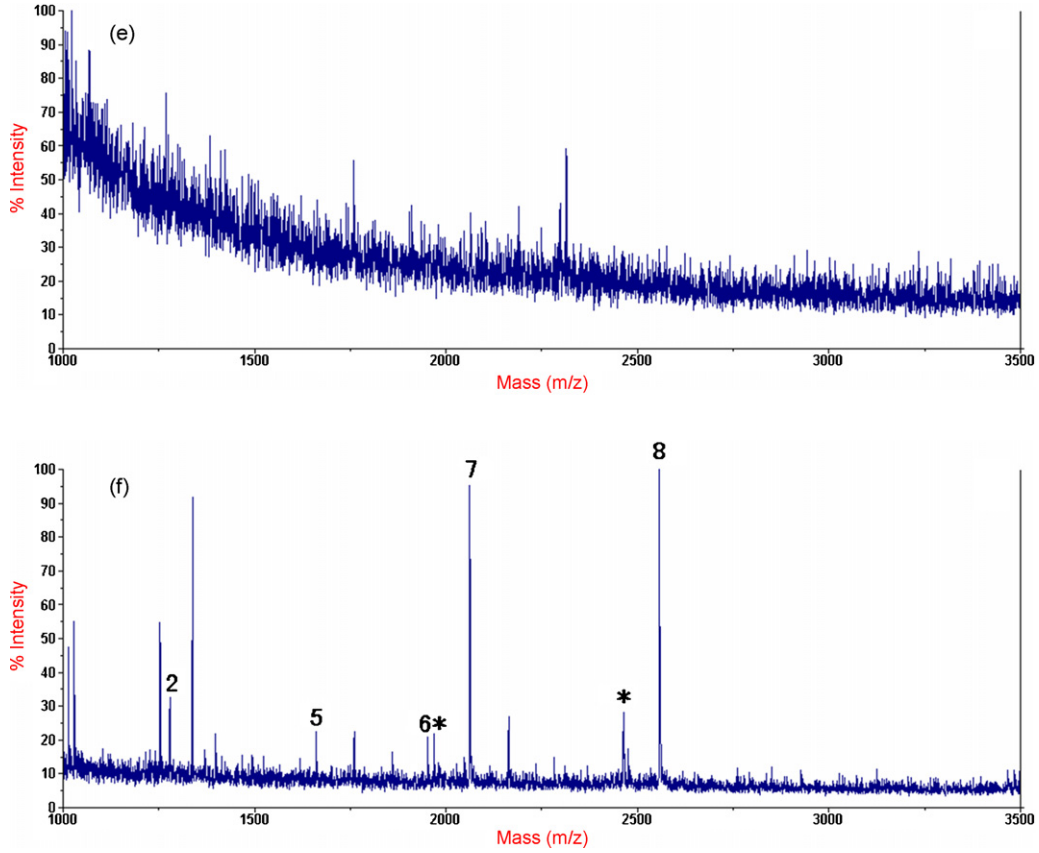

Fig. 4. (*Continued*).

low-pH solutions to achieve high phosphopeptide binding selectivity. However, both the pH and the ionic strength can influence binding properties. In Fig. 4b, 0.2% TFA solution was used as binding buffer. Although the non-specific binding of nonphosphorylated peptides was suppressed, the numbers of phosphopeptides identified and the intensities of the signals are still below expectation. Binding buffer consisting of 0.2% TFA and 50% ACN was used as a compromise of pH and ionic strength in Fig. 4d, almost all the peaks observed are related to phosphorylated peptides. The peaks 7, 8 and 9 (*m/z* 2061.8, 2556.1 and 3122.3) are derived from phosphopeptides of β-casein, while the peaks marked 3, 5 and 6 (*m/z* 1466.6, 1660.8 and 1952.0) are derived from phosphopeptides of α-casein due to the substoichiometric impurity present in β-casein. The peaks 1, 2 and 4 (*m/z* 1031.4, 1278.6 and 1561.7) could be attributed to the doubly charged ions of the three phosphopeptides 7, 8 and 9. This phenomenon has been reported previously [46,47]. Metastable loss of H_3PO_4 from parent ions during the fly procedure in TOF-tube can also be observed, which further supports the identification of phosphorylation in proteins. Peak 9 is the signal of a multiply phosphorylated peptide, therefore 3 peaks stand for metastable loss were detected.

Binding buffers contained increased TFA or ACN concentration was also tested as shown in Fig. 4e and f. Unfortunately, we observed decreased binding specificity and peak intensity under these circumstances. Neither increasing percentage of TFA nor ACN is helpful with specific binding of phosphorylated peptides according to the spectra. Therefore, solution contains of 0.2% TFA and 50% ACN is used as the binding buffer in following experiments.

3.3. Selective enrichment of phosphopeptides from peptide mixture using smooth and mesoporous TiO_2 microspheres

To establish how mesoporous TiO_2 phosphopeptide enrichment compares to smooth TiO_2 enrichment, we applied the protocol established above to both TiO_2 microspheres. Fig. 5 shows the MALDI mass spectrum of enriched tryptic digest of β-casein (1 ng/μL) using smooth TiO_2 microspheres. Almost all phosphopeptide signals including signals stand for metastable loss of H_3PO_4

Table 1
Detailed information of the observed phosphorylated peptides obtained from tryptic digestion of α-casein S1 and S2, and β-casein[a].

Peak number	Theoretical m/z	aa	Peptide sequence
1	1031.4	β/33–48	FQSEEQQQTEDELQDK
2	1278.6	β/33–52	FQSEEQQQTEDELQDKIHPF
3	1466.6	α-S2/153–164	TVDMSTEVFTK
4	1561.7	β/1–25	RELEELNVPGEIVESLSSSEESITR
5	1660.8	α-S1/106–119	VPQLEIVPNSAEER
6	1952.0	α-S1/104–119	YKVPQLEIVPNSAEER
7	2061.8	β/33–48	FQSEEQQQTEDELQDK
8	2556.1	β/33–52	FQSEEQQQTEDELQDKIHPF
9	3122.3	β/1–25	RELEELNVPGEIVESLSSSEESITR

[a] The phosphorylation sites are underlined.

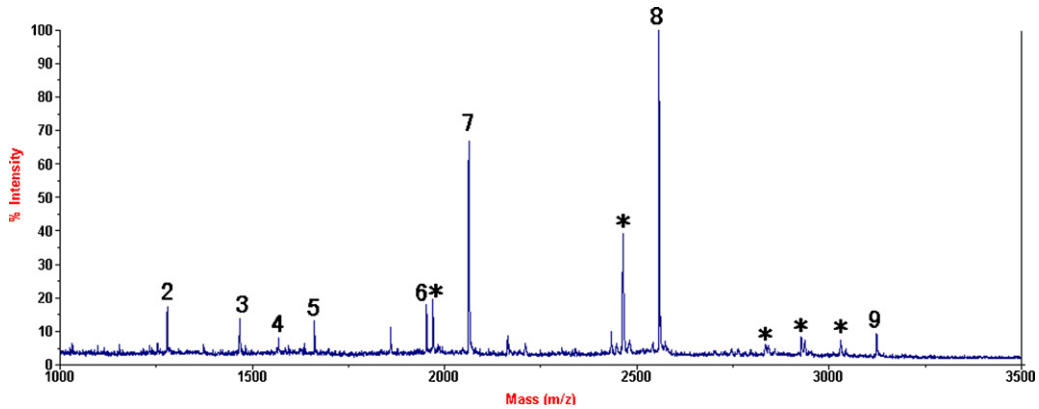

Fig. 5. Mass spectra obtained using the smooth amorphous TiO_2 microspheres to selectively enrich phosphorylated peptides from the tryptic digest of β-casein at concentration of 4.4×10^{-7} M. Phosphopeptides ions identified are marked with numbers. The metastable losses of phosphoric acid are indicated with asterisks.

and doubly charged ions derived from β-casein were successfully detected. Three phosphopeptide signals (peak 3, 5 and 6) derived from α-casein can also be observed. Enrichment of the digest generated from standard protein digestion shows little difference in phosphopeptide affinity between smooth and mesoporous TiO_2 microspheres, therefore, peptide mixtures containing of β-casein and BSA digestion with molar ratio of 1:1 and 1:10 were chosen as to test the selective enrichment ability of TiO_2 material with different surface structures. The concentration of β-casein was fixed at 4.4×10^{-7} M in the mixture. Fig. 6a and b represents the MALDI mass spectra obtained by phosphopeptides enrichment from the tryptic digest mixture containing β-casein and BSA at the molar ratio of 1:1 using smooth and mesoporous TiO_2 microspheres, respectively. In Fig. 6a, only three phosphopeptide ion signals (5, 7 and 8) are observed in the mass spectrum, the other abundant ion signals pertaining to nonphosphopeptides. In contrast, after enrichment by the mesoporous anatase TiO_2 microspheres, the signals related to phosphopeptides are highly enhanced and dominate the mass spectrum as shown in Fig. 6b. Three phosphorylated peptides (7, 8 and 9) of β-casein and three phosphopeptides (3, 5 and 6) of α-casein are clearly detected. The other peaks are assigned to doubly charged ions (1, 2 and 4) and dephosphorylated fragment ions. When the concentration of BSA was raised 10 times, only two phosphopeptides (7, 8) and one dephosphorylated fragment ions were detected by enrichment with smooth TiO_2 microspheres as shown in Fig. 6c. Most of signals in the spectrum are nonphosphopeptides. While using mesoporous TiO_2 microspheres, despite some nonspecific binding of acidic peptides such as the signal detected at *m/z* 1955.9 derived from BSA (S319-336, DAIPENLPPLTADFAEDK), phosphopeptides still dominate the mass spectrum (Fig. 6d). The observed difference in phosphopeptide binding selectivity between smooth and mesoporous TiO_2 microspheres could be related to their different surface areas. According to the BET data, the specific surface area of a mesoporous TiO_2 bead is almost 25 times of a smooth TiO_2 bead. The increasing surface area enhances the selectivity of TiO_2 microspheres towards phosphorylated peptides. There is no direct evidence regarding the influence of TiO_2 crystalline structure for phosphopeptide enrichment. However, Imami et al. [55] pointed out that rutile-form titania exhibited higher selectivity in phosphopeptide enrichment than commercial titania. Therefore, it is very possible that anatase-form of TiO_2 beads contribute to higher binding affinity with phosphorylated peptides than amorphous ones. The mesoporous anatase TiO_2 microspheres possess massive surface area, which make them perfect candidate for packing TiO_2 affinity chromatography in further study based on the experiment.

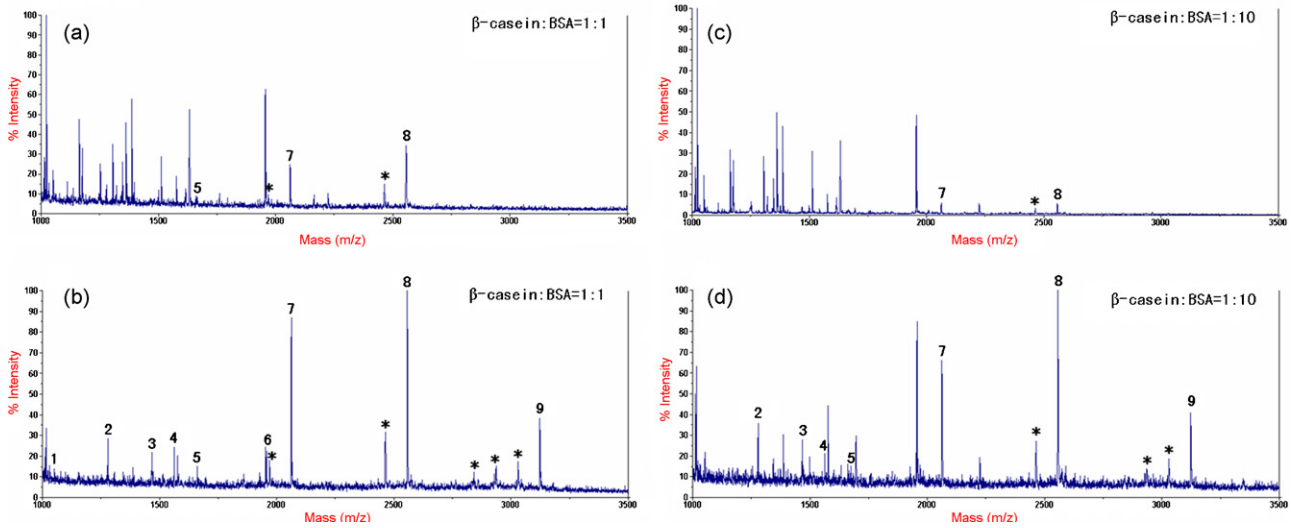

Fig. 6. Mass spectra obtained using the smooth amorphous (a, c) and mesoporous anatase (b, d) TiO_2 microspheres to selectively enrich phosphorylated peptides from the tryptic digest of β-casein and BSA with ratio of 1:1 and 1:10. All spectra were taken from signal-averaging of 800 laser shots with the laser intensity kept at a proper constant. Phosphopeptides ions identified are marked with numbers. The metastable losses of phosphoric acid are indicated with asterisks.

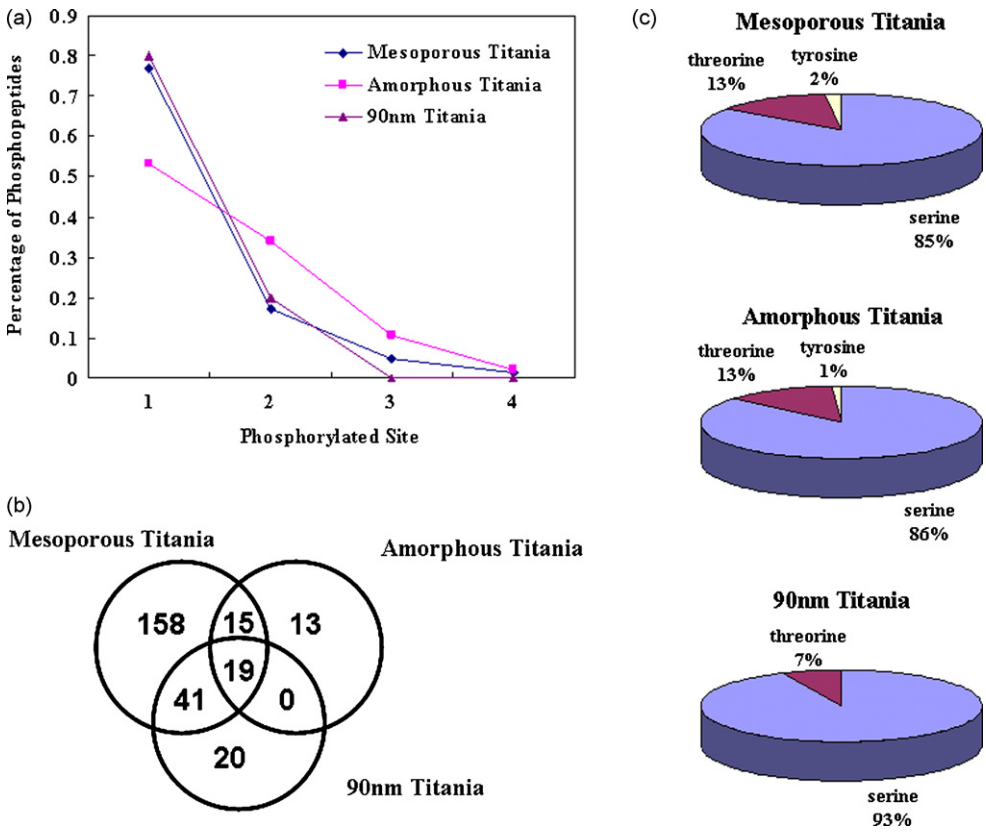

Fig. 7. (a) Phosphorylation states of peptides identified from rat brain tissue extract using mesoporous anatase titania, smooth amorphous titania and commercial 90 nm titania. (b) Comparison of the number of overlapping and unique phosphopeptide assignments obtained by enrichment using three kinds of TiO_2 particles of the global lysate extracted from rat brain tissue specimens. (c) Pie charts of the serine, threonine and tyrosine phosphorylation sites identified from rat brain tissue extract using mesoporous anatase titania, smooth amorphous titania and commercial 90 nm titania.

3.4. Selective enrichment of phosphopeptides from rat brain extracts using smooth, mesoporous, and commercial TiO_2 particles

To further reveal the divergence in phosphopeptide affinity between smooth and mesoporous TiO_2 microspheres, these two materials were applied to enrich phosphopeptides from tryptic digests of rat brain extract. The peptides eluted from both TiO_2 microspheres were analyzed by nano-RPLC-ESI-MS/MS/MS. A total number of 246 phosphopeptides were identified, in which 199 were identified independently by enrichment with mesoporous anatase TiO_2 microspheres, 13 were identified independently by enrichment with smooth amorphous TiO_2 microspheres, and 34 were identified by both materials. Commercial 90 nm TiO_2 nanospheres were also applied for phosphopeptides enrichment from the same sample. A total number of 80 phosphopeptides containing 96 phosphorylated sites were identified, and 20 unique peptides were observed. Though identified phosphopeptide amounts varied a lot, the distributions of phosphorylation sites on three amino acids are almost the same. Numbers of phosphopeptides and phosphorylated sites identified with three kinds of materials were also calculated and analyzed in Fig. 7a and b. There are 304 phosphorylation sites containing 259 on serine, 39 on threonine and 6 on tyrosine identified with mesoporous anatase TiO_2 microspheres, while only 76 phosphorylation sites containing 65 on serine, 10 on threonine and 1 on tyrosine were identified with smooth amorphous TiO_2 microspheres. In 96 phosphorylated sites identified by using commercial TiO_2 nanospheres, 89 of them were on serine and 7 were on threonine. No phosphorylated site was identified on tyrosine with commercial TiO_2 nanospheres. These data were presented as pie charts in Fig. 7c. The detailed informations of the phosphopeptides enriched by two materials were listed in supplementary Table 1 and supplementary Table 2. Monophosphorylated peptides account for more than half of the whole phosphopeptides identified using all three kinds of TiO_2 microspheres. It is probably because multiply phosphorylated peptides binding on the TiO_2 materials are difficult to elute due to their extremely high binding affinity [56]. Again, the trends of binding phosphopeptides with single or multiple phosphorylated sites are similar using these three materials. The enrichment divergence of the two TiO_2 microspheres with different surface structures provides evidence that greater surface area could lead to more efficient equilibrium between the particles and phosphopeptides during the loading and elution process. Moreover, the mesoporous TiO_2 microspheres possess a specific surface area even higher than commercial nano TiO_2 particles, which made them a promising candidate to be used as chromatographic materials.

4. Conclusions

TiO_2 is the most commonly used metal oxide for phosphopeptides enrichment. TiO_2 magnetic sphere or TiO_2 affinity chromatography has been reported a lot for phosphopeptides research. In this paper, we synthesized two kinds of TiO_2 microspheres with smooth and mesoporous surface [43]. The synthesis of these two materials is quite easy and low-cost. The specific surface area of the mesoporous TiO_2 microspheres is even higher than the commercial nano TiO_2 particles. Both of these two TiO_2 microspheres are successfully applied to selective enrichment of phosphopeptides generated from β-casein digest. However, when they are used for phosphopeptides enrichment from a complicated peptide mixture such as β-casein and BSA digest mixture,

mesoporous TiO_2 microspheres exhibit strong specific selectivity compared with amorphous TiO_2 microspheres with smooth surface. When they are further used for phosphopeptide enrichment from rat brain tissue extract, the mesoporous TiO_2 microspheres show a much higher binding capacity for phosphate groups as well as much higher capture efficiency for phosphopeptides compared with both the smooth amorphous TiO_2 microspheres and the commercial available TiO_2 nanoparticles. This mesoporous TiO_2 material may be further used as affinity chromatography column packing material for comprehensive phosphorylated proteome research.

Acknowledgements

We sincerely thank Dr. Wangjun Cui for his generous help with characterization of the materials. The work was supported by the National Basic Research Priorities Program (Project: 2007CB914100/3), the National Key Natural Science Foundation of China (Project: 20735005), the National Natural Science Foundation of China (Project: 20875017 and 30873132), and Shanghai Leading Academic Discipline Project (B109).

Appendix A. Supplementary data

Supplementary data associated with this article can be found, in the online version, at doi:10.1016/j.chroma.2010.02.008.

References

[1] J.D. Graves, E.G. Krebs, Pharmacol. Ther. 82 (1999) 111.
[2] T. Hunter, Cell 100 (2000) 113.
[3] H.K. Kweon, K. Håkansson, Anal. Chem. 78 (2006) 1743.
[4] D.T. McLachlin, B.T. Chait, Curr. Opin. Chem. Biol. 5 (2001) 591.
[5] M. Mann, S.E. Ong, M. Gronborg, H. Steen, O.N. Jensen, A. Pandey, Trends Biotechnol. 20 (2002) 261.
[6] R.E. Schweppe, C.E. Haydon, T.A. Lewis, K.A. Resing, N.G. Ahn, Acc. Chem. Res. 36 (2003) 453.
[7] M.J. Chalmers, W. Kolch, M.R. Emmett, A.G. Marshall, J. Chromatogr. B 803 (2004) 111.
[8] G.T. Cantin, J.R. Yates, J. Chromatogr. A 1053 (2004) 7.
[9] F. Meng, A.J. Forbes, L.M. Miller, N.L. Kelleher, Mass Spectrum Rev. 24 (2005) 57.
[10] D.C. Neville, C.R. Rozanas, E.M. Price, D.B. Gruis, A.S. Verkman, R.R. Townsend, Protein Sci. 6 (1997) 2436.
[11] M.C. Posewitz, P. Tempst, Anal. Chem. 71 (1999) 2883.
[12] T.S. Nuhse, A. Stensballe, O.N. Jensen, S.C. Peck, Mol. Cell. Proteomics 2 (2003) 1234.
[13] J.L. Wang, Y.J. Zhang, H. Jiang, Y. Cai, X.H. Qian, Proteomics 6 (2006) 404.
[14] H.J. Zhou, M.L. Ye ML, J. Dong, G.H. Han, et al., J. Proteome Res. 7 (2008) 3957.
[15] A. Pandey, A.V. Podtelejnikov, B. Blagoev, X.R. Bustelo, M. Mann, H.F. Lodish, Proc. Natl. Acad. Sci. U.S.A 97 (2000) 179.
[16] S.B. Ficarro, O. Chertihin, V.A. Westbrook, F. White, F. Jayes, P. Kalab, J.A. Marto, J. Shabanowitz, J.C. Herr, D.F. Hunt, P.E. Visconti, J. Biol. Chem. 278 (2003) 11579.
[17] H. Zhou, J.D. Watts, R. Aebersold, Nat. Biotechnol. 19 (2001) 375.
[18] D.T. McLachlin, B.T. Chait, Anal. Chem. 75 (2003) 6826.
[19] S.A. Beausoleil, M. Jedrychowski, D. Schwartz, J.E. Elias, J. Villen, J. Li, M.A. Cohn, L.C. Cantley, S.P. Gygi, Proc. Natl. Acad. Sci. U.S.A. 101 (2004) 12130.
[20] B.A. Ballif, J. Villen, S.A. Beausoleil, D. Schwartz, S.P. Gygi, Mol. Cell. Proteomics 3 (2004) 1093.
[21] M.W.H. Pinkse, P.M. Uitto, M.J. Hilhorst, B. Ooms, A.J.R. Heck, Anal. Chem. 76 (2004) 3935.
[22] S.H. Sui, J.L. Wang, B. Yang, et al., Proteomics 8 (2008) 2024.
[23] G.H. Han, M.L. Ye, H.J. Zhou, X.N. Jiang, et al., Proteomics 8 (2008) 1346.
[24] M.R. Larsen, T.E. Thingholm, O.N. Jensen, P. Roepstorff, T.J.D. Jorgensen, Mol. Cell. Proteomics 4 (2005) 873.
[25] D.W. Qi, J. Lu, C.H. Deng, J. Phys. Chem. C 113 (2009) 15854.
[26] H.K. Kweon, K. Hakansson, Anal. Chem. 78 (2006) 1743.
[27] C.Y. Lo, W.Y. Chen, C.T. Chen, Y.C. Chen, J. Proteom. Res. 6 (2007) 887.
[28] D.W. Qi, J. Lu, C.H. Deng, J. Chromatogr. A 1216 (2009) 5533.
[29] F. Wolschin, S. Wienkoop, W. Weckwerth, Proteomics 5 (2005) 4389.
[30] C.T. Chen, W.Y. Chen, P.J. Tsai, K.Y. Chien, J.S. Yu, Y.C. Chen, J. Proteome Res. 6 (2007) 316.
[31] H.J. Zhou, R.J. Tian, M.L. Ye, S.Y. Xu, Electrophoresis 28 (2007) 2201.
[32] S. Xu, J.C. Whitin, T.T. Yu, H. Zhou, D. Sun, H. Sue, H. Zou, H.J. Cohen, R.N. Zare, Anal. Chem. 80 (2008) 5542.
[33] C.S. Pan, M.L. Ye, Y.G. Liu, S. Feng, et al., J. Proteome Res. 5 (2006) 3114.
[34] Y. Li, D. Qi, C. Deng, P. Yang, X. Zhang, J. Proteome Res. 7 (2008) 1767.
[35] Y. Li, T. Leng, H. Lin, C. Deng, et al., J. Proteome Res. 6 (2007) 4498.
[36] Y. Li, J. Wu, C. Deng, et al., Chem. Commun. 46 (2008) 564.
[37] Y. Li, Y. Liu, J. Tang, H. Lin, N. Yao, X. Shen, C. Deng, P. Yang, X. Zhang, J. Chromatogr. A 1172 (2007) 57.
[38] Y. Li, X. Xu, D. Qi, C.H. Deng, J. Proteome Res. 7 (2008) 2526.
[39] Y. Ikeguchi, H. Nakamura, Anal. Sci. 16 (2000) 541.
[40] Z.T. Jiang, Y.M. Zuo, Anal. Chem. 73 (2001) 686.
[41] M. Kawahara, H. Nakamura, T. Nakajima, J. Chromatogr. 515 (1990) 149.
[42] A. Sano, H. Nakamura, Anal. Sci. 20 (2004) 565.
[43] S.S. Jensen, M.R. Larsen, Rapid Commun. Mass Spectrom. 21 (2007) 3635.
[44] S. Mohammed, K. Kraiczek, M.W. Pinkse, S. Lemeer, J.J. Benschop, A.J. Heck, J. Proteome Res. 7 (2008) 1565.
[45] S.S. Liang, H. Makamba, S.Y. Huang, S.H. Chen, J. Chromatogr. A 1116 (2006) 38.
[46] C.T. Chen, Y.C. Chen, Anal. Chem. 77 (2005) 5912.
[47] F. Torta, M. Fusi, C.S. Casari, C.E. Bottani, A. Bachi, J. Proteome Res. 8 (2009) 1932.
[48] W.Q. Shui, J. Fan, P.Y. Yang, Anal. Chem. 78 (2006) 4811.
[49] R.J. Tian, H. Zhang, M.L. Ye, H.F. Zou, et al., Angew. Chem. Inter. Ed. 46 (2007) 962.
[50] P.Y. Wang, L. Zhao, R. Wu, H. Zhong, et al., J. Phys. Chem. C 113 (2009) 1359.
[51] J.Y. Yan, X.L. Li, S.Y. Cheng, Y.X. Ke, X.M. Liang, Chem. Commun. 20 (2009) 2929.
[52] D. Chen, F. Huang, Y. Cheng, R.A. Caruso, Adv. Mater. 21 (2009) 2206.
[53] A. Keller, A.I. Nesvizhskii, E. Kolker, R. Aebersold, Anal. Chem. 74 (2002) 5383.
[54] K.A. Kraus, H.O. Philips, T.A. Carlson, J.S. Johnson, Proceedings of the Second International Conference on Peaceful Uses of Atomic Energy, Geneva, Switzerland, 1958, p. 3.
[55] K. Imami, N. Sugiyama, Y. Kyono, et al., Anal. Sci. 24 (2008) 161.
[56] T.E. Thingholm, O.N. Jensen, P.J. Robinson, M.R. Larsen, Mol. Cell. Proteomics 6 (2007) 1392.